PROTEIN STRUCTURE REPORT

Crystal structure of the C-terminal domain of the *Salmonella* type III secretion system export apparatus protein InvA

Liam J. Worrall, Marija Vuckovic, and Natalie C. J. Strynadka*

Centre for Blood Research, Department of Biochemistry and Molecular Biology, University of British Columbia, Life Sciences Centre, British Columbia, Canada V6T 1Z3

Received 1 March 2010; Revised 3 March 2010; Accepted 3 March 2010
DOI: 10.1002/pro.382
Published online 19 March 2010 proteinscience.org

Abstract: InvA is a prominent inner-membrane component of the *Salmonella* type III secretion system (T3SS) apparatus, which is responsible for regulating virulence protein export in pathogenic bacteria. InvA is made up of an N-terminal integral membrane domain and a C-terminal cytoplasmic domain that is proposed to form part of a docking platform for the soluble export apparatus proteins notably the T3SS ATPase InvC. Here, we report the novel crystal structure of the C-terminal domain of *Salmonella* InvA which shows a compact structure composed of four subdomains. The overall structure is unique although the first and second subdomains exhibit structural similarity to the peripheral stalk of the A/V-type ATPase and a ring building motif found in other T3SS proteins respectively.

Keywords: type III secretion; Salmonella; crystal structure; InvA

Introduction

The bacterial injectisome, or nonflagellar type III secretion system (NF-T3SS), is a specialized needle-like protein-export system utilized by many pathogenic or symbiotic Gram-negative bacteria for the injection of virulence inducing proteins (effectors) into host cells. It is essential for the virulence of many medically relevant bacteria including *Pseudomonas, Yersinia, Salmonella, Shigella* and enteropathogenic *E. coli* (EPEC). Bacterial proteins destined for both needle assembly and host cell targeting are translocated via the injectisome in a process known as type III secretion. This process has characteristics in common with the assembly of the flagellar motility machinery (F-T3SS) of bacteria and there exists extensive homology between these two systems particularly within the inner membrane components.

Indispensable for secretion are a set of highly conserved inner membrane proteins believed to be located in the pore at the base of the injectisome (SpaPQRS+InvA, *Salmonella* nomenclature; YscR-STUV, *Yersinia* nomenclature; FliO(no NF-T3SS homologue)PQR+FlhBA, flagellar nomenclature) and several membrane associated proteins most notably the type III ATPase InvC/YscN/FliI (*Salmonella*/*Yersinia*/flagellar). The membrane components are predicted to form an export channel with the cytoplasmic domains of SpaS/YscU/FlhB and InvA/YscV/

Grant sponsors: Canadian Commonwealth Scholarship Program, Canadian Institutes for Health Research, Howard Hughes Medical Institute International Scholar program, Canada Foundation for Innovation, Michael Smith Foundation for Health Research.

*Correspondence to: Natalie C. J. Strynadka, Centre for Blood Research, Department of Biochemistry and Molecular Biology, University of British Columbia, Life Sciences Centre, British Columbia, Canada V6T 1Z3. E-mail: natalie@byron.biochem.ubc.ca

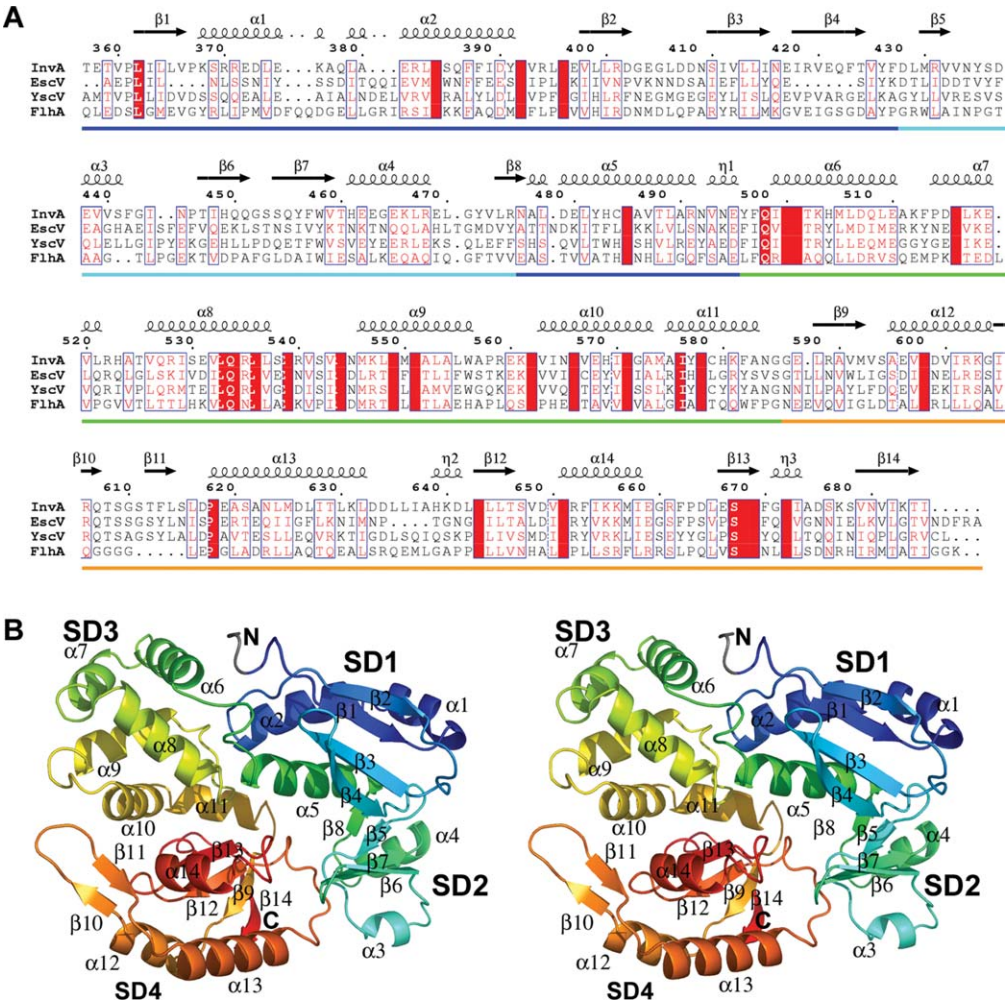

Figure 1. Structure of InvA$_{357–685}$. (a) Sequence alignment of InvA$_{357–685}$ and homologues from *EPEC* (EscV), *Yersinia* (YscV) and the *Salmonella* F-T3SS (FlhA). Secondary structure from InvA structure depicted above. Subdomains indicated along bottom (SD1–blue; SD2–cyan; SD3–green; SD4–orange). (b) Stereo diagram of overall structure of InvA$_{357–685}$. Colored from N-terminal (blue) to C-terminal (red) (N-terminal tag gray). All structural figures were prepared with PyMOL.[9]

FlhA acting as a docking platform for the substrate bound InvC/YscN/FliI complex.[1] Upon binding, InvC/YscN/FliI is proposed to use the energy derived from ATP hydrolysis to dissociate substrate-chaperone complexes[2] before translocation through the T3SS in a process driven by the proton motive force.[3,4]

InvA/YscV/FlhA, the largest member of the inner membrane export apparatus, consists of a highly conserved ~35 kDa N-terminal integral membrane region connected by a 20–30 residue flexible linker to a more variable ~40 kDa C-terminal soluble domain proposed to be localized to the bacterial cytoplasm. The paralogous C-terminal domain of *Salmonella* flagellar FlhA [~22% sequence identity with the C-terminal domain of InvA; Fig. 1(a)] has been studied using a variety of biochemical and cellular approaches. It has been shown to interact with several soluble flagellar apparatus proteins including the ATPase FliI (InvC/YscN), its regulator FliH (OrgB/YscL), and FliJ (InvI/YscO); and is associated with a dominant-negative multicopy effect, inhibiting flagellar action by sequestering soluble components of the assembly apparatus in non-productive complexes.[1,5-8] It is proposed that the C-terminal domain of FlhA provides one of the main sites of interaction at the base of the F-T3SS for the soluble assembly complex before subsequent substrate insertion into the inner membrane portal of the F-T3SS.[7]

Structural data for the conserved core inner membrane components of the T3SS export apparatus is limited to the C-terminal cytoplasmic domain of SpaS/YscU/FlhB from several NF-T3SS homologues[10-13] and the ATPase from both NF-T3SS[14] and F-T3SS[15] homologues. To gain insight into the function of InvA/YscV/FlhA we have solved the first representative structure of this family, the C-terminal domain of NF-T3SS *Salmonella enterica* serovar Typhimurium InvA.

Results and Discussion

Structure determination

The structure of the C-terminal domain of *S. enterica* serovar Typhimurium InvA (InvA$_{357–685}$) from the *Salmonella* pathogenicity island 1 (SPI-1) was

Table I. *Data Collection and Refinement Statistics. Values in Parenthesis Are for Highest-Resolution Shell. Data Refined Against a High-Resolution Dataset Collected at the Remote Wavelength and Merged with the "Remote" Dataset (HR-Rem-mrg)*

	Form 1					
Data collection	Remote	HR-Rem-mrg	Peak	Inflection 1	Inflection 2	Form 2
Space group			$P2_12_12_1$			$P3_221$
Cell dimensions						
a,b,c (Å)			44.8, 57.3, 113.6			79.2, 79.2, 127.7
α,β,γ (°)			90, 90, 90			90, 90, 120
Wavelength (Å)		0.9793	1.0064	1.0087	1.0084	1.5418
Resolution (Å)	50–2.2 (2.31–2.2)	30–1.5 (1.57–1.5)	50–2.2 (2.31–2.2)	50–2.2 (2.31–2.2)	50–2.2 (2.31–2.2)	68–2.5 (2.65–2.5)
R_{merge} (%)	4.2 (6.9)	10.5 (22.5)	4.1 (9.7)	2.9 (4.1)	3.1 (6.4)	6.5 (23.2)
Average I/σ(I)	28.7 (15.8)	11.4 (2)	20.7 (7.7)	29.1 (15.5)	26.5 (13)	12.6 (4.0)
Completeness (%)	97.2 (97.2)	93.3 (93.3)	89.7 (89.7)	88.9 (88.9)	89.5 (89.5)	96.5 (76.2)
Redundancy	6.1 (3.2)	4.5 (1.9)	3.4 (1.9)	3.4 (1.9)	3.4 (1.9)	4.3 (4.1)
Refinement						
Resolution (Å)		30–1.5 (1.57–1.5)				68–2.5 (2.65–2.5)
No. reflections		202976 (9403)				67747 (7252)
Unique reflections		44795 (4823)				15695 (1764)
R/R_{free}[a] (%)		19.2/22.5				20.6/26.4
No. atoms						
Protein		2691				2648
Water		292				78
Other		12				24
B-factors (Å^2)						
Protein		19.17				22.2
Water		31.52				20.6
Other		38.72				52.4
r.m.s. deviations						
Bond lengths (Å)		0.0173				0.0201
Bond angles (°)		1.651				1.812
Ramachandran plot (%)						
Favored		98.5				95.36
Allowed		2.5				4.33
Disallowed		0				0.31

[a] 5% of data used for R_{free} calculation.

determined to 1.5 Å resolution. The protein crystallized in two crystal forms with space groups $P2_12_12_1$ and $P3_221$, both with one molecule in the asymmetric unit (for data collection and refinement statistics see Table I). Phases were experimentally determined from form 1 crystals using multiple wavelength anomalous dispersion with an ethyl mercury phosphate derivative. Three heavy-atom positions were located bound to residues His^{461}, Cys^{474}, and Cys^{579}. The phases for the native data collected from form 2 crystals were solved using molecular replacement with the form 1 structure as a search model. The refined structures have good overall stereochemistry and are in good agreement with a backbone RMSD of 0.8 Å. In addition to the heavy atoms, two calcium atoms and a PEG molecule have been modelled in the form 1 data and two phosphates and one CAPS molecule included in the form 2 model.

Overall structure of InvA$_{357–685}$

The overall structure shows a relatively compact globular fold with approximate dimensions of 60 × 50 × 40 Å, that can be divided into four subdomains referred to as InvA$_{357–685}$SD1–4 [Fig. 1(b)]. InvA$_{357–685}$SD1 is made of two segments, residues (−4)357–427 and 476–496 (−4 to −1 denote remnant tag residues), and is composed of three helices and four sheets. The central core of the domain is made up of a mixed four stranded beta-sheet in a 1X −2 −1 topology,[16] which is packed against three helices in a topological arrangement of β_1, α_1, α_2, β_2, β_3, β_4, α_5. The majority of secondary structure elements are at the N-terminus whilst helix α_5 is situated in sequence following InvA$_{357–685}$SD2. Helix α_5 kinks sharply ~90° at the C-terminal ending in a three residue 3_{10}-helix that forms part of the interface with InvA$_{357–685}$SD3. There is a slight variation in the N-terminal region between crystal forms 1 and 2 with the first six residues incorporating the four left over tag residues and residues 357–358 not visible in the form 2 electron density despite being well ordered in the form 1 model.

InvA$_{357–685}$SD2 (residues 428–475) is the smallest subdomain. It is a mixed α/β subdomain consisting of a four stranded antiparallel β-sheet with −2X 1 2X topology. Helices α3 and α4 pack against the

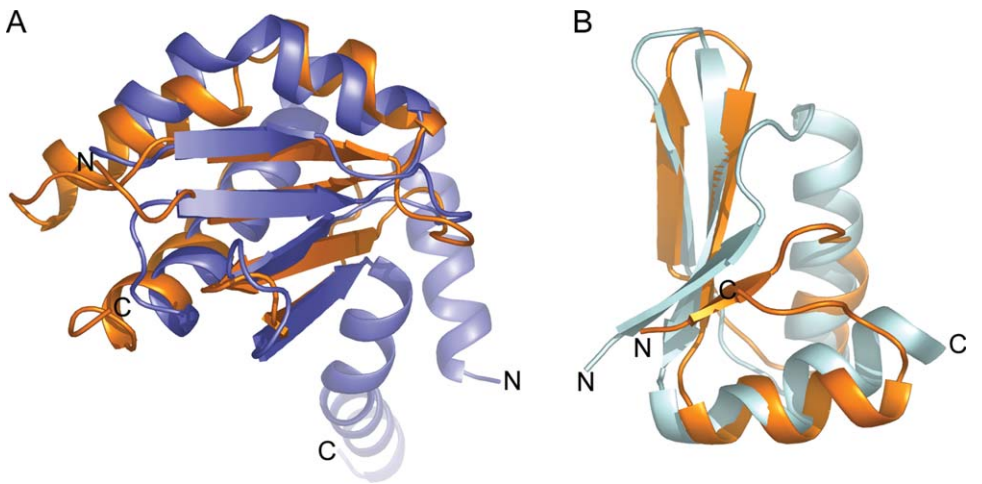

Figure 2. Structural similarity of $InvA_{357–685}SD1$ and $InvA_{357–685}SD2$. (a) Structural alignment of $InvA_{357–685}SD1$ (orange) and subunit E of the A-ATPase peripheral stalk (blue, PDB 2DM9). DALI Z-score 2.7, RMSD 2.5 Å. (b) Structural alignment of $InvA_{357–685}SD2$ (orange) and a ring building domain from EscJ (cyan, PDB 1YJ7). DALI Z-score 4.0, RMSD 1.8 Å.

β-sheet to form a wedge shaped fold with the β-hairpin formed by β6 and β7 projecting toward and contacting $InvA_{357–685}SD4$. $InvA_{357–685}SD3$ (residues 476–585) is an all helical subdomain composed of six helices (α6-α11) positioned in an anticlockwise arrangement. $InvA_{357–685}SD4$ (residues 586–685) is composed of three α-helices and six β-strands. Four strands (β9, β12–14) form a parallel β-sheet with 1X 1X −3X topology, which is flanked by helix α14 and the N- and C-terminal ends of helices α12 and α13 on one side and two 3_{10}-helices on the other. Strands β10 and β11 comprise an extended β-hairpin protruding from helices α12 and α13 that reaches up to and contacts the N-terminal end of helix α10 from SD3. This motif, in particular residues Arg^{606} to Thr^{612} exhibits the most significant degree of structural variability between the two crystal forms with up to a 4 Å shift away from SD3 observed in form 2. This is associated with significantly higher than average backbone temperature factors in both models indicative of a degree of conformational flexibility for this region of the protein.

The overall structure is relatively compact and there are extensive inter-subdomain interactions within the fold. $InvA_{357–685}SD1$ interacts with each subdomain forming interfaces of 471, 666, and 180 $Å^2$ with subdomains 2, 3, and 4 respectively. In addition to $InvA_{357–685}SD1$, $InvA_{357–685}SD2$ also interacts with $InvA_{357–685}SD4$ with an interface area of 480 $Å^2$. The largest interface is between $InvA_{357–685}SD3$ and $InvA_{357–685}SD4$ with an area of 782 $Å^2$.

Structural comparisons

A structural similarity search of the Protein Data Bank with the pairwise structural comparison server DALI[17] of the complete InvA C-terminal domain gave no statistically significant global similarities. Searching with the individual subdomains revealed that the overall architecture of $InvA_{357–685}SD1$ is that of a canonical thioredoxin/glutaredoxin-like fold with the highest Z-score to an annotated thioredoxin of 5.5 (PDB 1V98) with a core RMSD of 2.6 Å. However, the catalytic cysteine residues at the beginning of thioredoxin helix α3 are not conserved and helix α2 of the thioredoxin fold is absent. Of notable interest is a predicted similarity to the E subunit of the peripheral stalk from the archeal A_0A_1 ATP synthase (Z-score 2.7, core RMSD 2.5 Å, PDB 2DM9) [Fig. 2(a)]. Connectivity is conserved for the core of the fold although helix α5 of $InvA_{357–685}SD1$, situated in sequence following $InvA_{357–685}SD2$, superposes with an N-terminal helix from subunit E. F/V/A-type ATPases are related rotary motors that link transmembrane ion transport with ATP metabolism. They are composed of a catalytic soluble component ($F/V/A_1$) and a membrane bound ion channel ($F/V/A_0$) and the peripheral stalk links the two, acting as a stator to prevent unwanted rotation of the catalytic subunits. The E subunit of the A- and V-ATPases has a globular C-terminal domain, similar in structure to $InvA_{357–685}SD1$, which interacts with the N-terminal domain of the noncatalytic B subunit of the A/V_1 component.[19] The related catalytic/non-catalytic subunits of the F/V/A-type ATPases (α/β in the F-ATPase and A/B in the V/A-ATPase) are close structural homologues of the T3SS/flagellar ATPase[14,15] and other homologues between the T3SS and F/V/A-ATPases have been observed.[17] In light of the ability of the C-terminal domain of flagellar FlhA to interact with the F-T3SS ATPase, this observed structural similarity to a protein capable of binding a homologous ATPase may reflect a common mode of interaction for InvA/YscV/FlhA and the ATPase InvC/YscN/FliI although such a hypothesis requires experimental validation.

The highest scoring annotated DALI hit for $InvA_{357–685}$SD2 is surprisingly to a domain from EscJ (Z-score 4.0, RMSD 1.8 Å, PDB 1YJ7) [Fig. 2(b)], another component of the *EPEC* T3SS. EscJ is highly conserved and homo-oligomerises to form the prominent inner membrane ring of the T3SS basal body.[20] Despite lack of detectable sequence conservation, the same domain has recently been observed in two further ring forming T3SS basal body components: *Salmonella* PrgH, which forms a ring structure that encompasses *Salmonella* EscJ homologue PrgK; and *EPEC* EscC, a member of the highly conserved secretin family that forms the sole outer membrane ring. In addition, the motif is also found in GspD, a type II secretion system secretin.[21] It is proposed that this topologically similar fold provides a flexible ring building motif.[22] Although F-T3SS InvA homologue FlhA has been shown to interact with itself[5] it has not been shown to form any large stable homomeric complexes in solution as supported by our observations from static light scattering analysis of $InvA_{357–685}$ at various concentrations (data not shown). The discovery of this motif in an additional member of the T3SS is thus of interest and warrants further investigation into the role of oligomerization in the InvA/YscV/FlhA family with particular focus on the membrane anchoring region and other inner membrane components that may potentiate self-association. Additionally, a similar domain from *P. aeruginosa* Rhomboid was shown to mediate membrane association.[23] Since the C-terminal domain is tethered to the transmembrane N-terminal region it is possible that this subdomain plays some role in peripheral membrane association.

$InvA_{357–685}$SD3 and SD4 yield multiple significant hits including domains within the ribonucleotide reductase R1 protein (Z-score 5.9) and a tRNA 2-selenouridine synthase (Z-score of 4.5) respectively although the specific function of the similar domains in all cases is not specifically understood.

Materials and Methods

Expression, purification, and crystallization

His_6-tagged $InvA_{357–685}$ was expressed from a pET-28a plasmid in BL21 cells for 4 h at 37°C. The protein was purified using Ni^{2+} charged fast-flow chelating sepharose (GE Healthcare), dialyzed overnight against 20 m*M* tris pH 7.5, 50 m*M* NaCl, 0.5 m*M* TCEP in the presence of thrombin (HTI) and resolved on a Superdex 200 16/60 (GE Healthcare) equilibrated in the same buffer. Protein was concentrated to 5–10 mg/mL. Crystals were grown at 293 K by sitting-drop vapor diffusion using either 15–20% PEG 500, 0.05 *M* $CaCl_2$, 0.1 *M* citrate pH 5.5 (form 1) or 0.2 *M* $LiSO_4$, 0.1 *M* CAPS (*N*-cyclohexyl-3-aminopropanesulfonic acid) pH 10.5, 1.2 *M* NaH_2PO_4/0.8 *M* K_2HPO_4 (form 2) as reservoir solution.

Data collection and structure determination

Form 1 crystals were cryo-protected by increasing the concentration of PEG 500 to 25% and form 2 crystals were cryo-protected by supplementing the reservoir solution with 20% ethylene glycol. An ethyl mercuric phosphate derivative of form 1 crystals was obtained by soaking in cryo-protectant +2 m*M* ethyl mercury phosphate for 1 h. A four wavelength MAD experiment[24] was carried out at beamline ID08–1 of the Canadian Light Source (Saskatoon, Canada) at 100 K. A high resolution dataset was also collected from the same crystal at 0.9793 Å and merged with the high-energy remote. Native data were collected from form 2 crystals on a rotating anode in-house X-ray generator at 100 K. All data were indexed and integrated using the MOSFLM package[25] and scaled using SCALA.[26] Substructure determination and phasing was carried out with autoSHARP,[27] finding three heavy atoms and yielding excellent phasing statistics and a high quality initial map. Automatic model-building was carried using ARP/wARP.[26] Iterative model building and refinement, using the high-resolution dataset, was carried out with COOT[28] and REFMAC[26] using TLS refinement[29] in the later stages with a final R/R_{free} of 19.2/22.5%. Data collected from form 2 crystals was phased by molecular replacement with the program PHASER[26] using the form 1 structure as a search model and refined with the same protocol to a final R/R_{free} of 20.6/26.4%. Data processing and model refinement statistics are summarized in Table I. Structure quality was assessed with MolProbity[30] and the final analysis results were included in the file deposited to the Protein Data Bank.

Accession numbers

The structure factors and coordinates have been deposited in the Protein Data Bank under accession codes 2X49 and 2X4A.

Conclusions

In conclusion, we have solved the high resolution crystal structure of the C-terminal cytoplasmic domain of the NF-T3SS export apparatus protein InvA. This is the first structural information of the InvA/YscV/FlhA family and adds to the increasing structural knowledge of the conserved core inner membrane T3SS export apparatus proteins. The structural similarities observed between InvA and the ATPase binding peripheral stalk from the A/V-type ATPases and a proposed ring building motif from other T3SS proteins may be a basis for functional comparison and merit further investigation into the functional interactions of the InvA/YscV/FlhA family.

Acknowledgment

Part of this research was performed at the Canadian Light Source, which was supported by NSERC, NRC, CIHR, and the University of Saskatchewan.

References

1. Minamino T, Macnab RM (2000) Interactions among components of the *Salmonella* flagellar export apparatus and its substrates. Mol Microbiol 35:1052–1064.
2. Akeda Y, Galan JE (2005) Chaperone release and unfolding of substrates in type III secretion. Nature 437:911–915.
3. Minamino T, Namba K (2008) Distinct roles of the FliI ATPase and proton motive force in bacterial flagellar protein export. Nature 451:485–488.
4. Paul K, Erhardt M, Hirano T, Blair DF, Hughes KT (2008) Energy source of flagellar type III secretion. Nature 451:489–492.
5. Zhu K, Gonzalez-Pedrajo B, Macnab RM (2002) Interactions among membrane and soluble components of the flagellar export apparatus of *Salmonella*. Biochemistry 41:9516–9524.
6. Mcmurry JL, Van Arnam JS, Kihara M, Macnab RM (2004) Analysis of the cytoplasmic domains of *Salmonella* FlhA and interactions with components of the flagellar export machinery. J Bacteriol 186:7586–7592.
7. Saijo-Hamano Y, Minamino T, Macnab RM, Namba K (2004) Structural and functional analysis of the C-terminal cytoplasmic domain of FlhA, an integral membrane component of the type III flagellar protein export apparatus in *Salmonella*. J Mol Biol 343:457–466.
8. Gonzalez-Pedrajo B, Minamino T, Kihara M, Namba K (2006) Interactions between C ring proteins and export apparatus components: a possible mechanism for facilitating type III protein export. Mol Microbiol 60:984–998.
9. Delano WL (2008) The PyMOL molecular graphics system. CA: DeLano Scientific LLC.
10. Deane JE, Graham SC, Mitchell EP, Flot D, Johnson S, Lea SM (2008) Crystal structure of Spa40, the specificity switch for the *Shigella flexneri* type III secretion system. Mol Microbiol 69:267–276.
11. Zarivach R, Deng W, Vuckovic M, Felise HB, Nguyen HV, Miller SI, Finlay BB, Strynadka NC (2008) Structural analysis of the essential self-cleaving type III secretion proteins EscU and SpaS. Nature 453:124–127.
12. Lountos GT, Austin BP, Nallamsetty S, Waugh DS (2009) Atomic resolution structure of the cytoplasmic domain of *Yersinia pestis* YscU, a regulatory switch involved in type III secretion. Protein Sci 18:467–474.
13. Wiesand U, Sorg I, Amstutz M, Wagner S, Van Den Heuvel J, Luhrs T, Cornelis GR, Heinz DW (2009) Structure of the type III secretion recognition protein YscU from *Yersinia enterocolitica*. J Mol Biol 385: 854–866.
14. Zarivach R, Vuckovic M, Deng W, Finlay BB, Strynadka NC (2007) Structural analysis of a prototypical ATPase from the type III secretion system. Nat Struct Mol Biol 14:131–137.
15. Imada K, Minamino T, Tahara A, Namba K (2007) Structural similarity between the flagellar type III ATPase FliI and F1-ATPase subunits. Proc Natl Acad Sci USA 104:485–490.
16. Richardson JS (1977) Beta-sheet topology and the relatedness of proteins. Nature 268:495–500.
17. Pallen MJ, Bailey CM, Beatson SA (2006) Evolutionary links between FliH/YscL-like proteins from bacterial type III secretion systems and second-stalk components of the FoF1 and vacuolar ATPases. Protein Sci 15: 935–941.
18. Holm L, Kaariainen S, Rosenstrom P, Schenkel A (2008) Searching protein structure databases with DaliLite v.3. Bioinformatics 24:2780–2781.
19. Lokanath NK, Matsuura Y, Kuroishi C, Takahashi N, Kunishima N (2007) Dimeric core structure of modular stator subunit E of archaeal H+ -ATPase. J Mol Biol 366:933–944.
20. Yip CK, Kimbrough TG, Felise HB, Vuckovic M, Thomas NA, Pfuetzner RA, Frey EA, Finlay BB, Miller SI, Strynadka NC (2005) Structural characterization of the molecular platform for type III secretion system assembly. Nature 435:702–707.
21. Korotkov KV, Pardon E, Steyaert J, Hol WG (2009) Crystal structure of the N-terminal domain of the secretin GspD from ETEC determined with the assistance of a nanobody. Structure 17:255–265.
22. Spreter T, Yip CK, Sanowar S, Andre I, Kimbrough TG, Vuckovic M, Pfuetzner RA, Deng W, Yu AC, Finlay BB, Baker D, Miller SI, Strynadka NC (2009) A conserved structural motif mediates formation of the periplasmic rings in the type III secretion system. Nat Struct Mol Biol 16:468–476.
23. Del Rio A, Dutta K, Chavez J, Ubarretxena-Belandia I, Ghose R (2007) Solution structure and dynamics of the N-terminal cytosolic domain of rhomboid intramembrane protease from Pseudomonas aeruginosa: insights into a functional role in intramembrane proteolysis. J Mol Biol 365:109–122.
24. Ji X, Blaszczyk J, Chen X (2001) The absorption edge of protein-bound mercury and a double-edge strategy for HgMAD data acquisition. Acta Cryst 57:1003–1007.
25. Leslie AGW (1992) Recent changes to the MOSFLM package for processing film and image plate data. Joint CCP4 + ESF-EAMCB Newsletter Protein Crystallogr 26.
26. CCPR (1994)The CCP4 suite: programs for protein crystallography. Acta Cryst 50:760–763.
27. Vonrhein C, Blanc E, Roversi P, Bricogne G (2007) Automated structure solution with autoSHARP. Methods Mol Biol 364:215–230.
28. Emsley P, Cowtan K (2004) Coot: model-building tools for molecular graphics. Acta Cryst 60:2126–2132.
29. Winn MD, Isupov MN, Murshudov GN (2001) Use of TLS parameters to model anisotropic displacements in macromolecular refinement. Acta Cryst 57:122–133.
30. Davis IW, Leaver-Fay A, Chen VB, Block JN, Kapral GJ, Wang X, Murray LW, Arendall WB, Snoeyink J, Richardson JS, Richardson DC (2007) MolProbity: all-atom contacts and structure validation for proteins and nucleic acids. Nucl Acids Res 35:W375–W383.